Study of a hot plate heating for spray CVD deposition on glass substrates

Pierre-Olivier Logerais, Olivier Riou, Vincent Froger, Anne Bouteville

Study of a hot plate heating for spray CVD deposition on glass substrates

by P.O. Logerais*, O. Riou*, V. Froger** and A. Bouteville**

*CERTES, IUT de Sénart, Université Paris-Est, 77127 Lieusaint (France), pierre-olivier.logerais@u-pec.fr
**LAMPA, Arts et Métiers ParisTech, 49035 Angers (France), anne.bouteville@angers.ensam.fr

Abstract

A thermographic approach is used to determine the temperature of an aluminium nitride hot plate as a glass substrate heater for depositing thin films by spray CVD (Chemical Vapour Deposition). The true temperature of the hot plate is determined by measuring its emissivity and the background temperature. The emissivity is found by means of a commercial infrared camera in the temperature range of [40°C, 540°C] with a better than 3% accuracy. The measured thermographic values are then corrected with a temperature precision of less than 4% for the highest temperatures considered. Moreover, the temperature profiles are plotted and good temperature homogeneity is observed.

1. Introduction

Spray CVD (Chemical Vapour Deposition) is a thin film deposition technique where fine liquid droplets are projected onto a heated glass substrate [1]. With this method, coatings for solar cells such as Transparent Conducting Oxides (TCO) can be deposited in a cheap way [2,3]. However, one of the remaining challenges is to have a uniform substrate temperature in order to get homogeneous thin film deposition. Consequently, the heating of the glass substrate has to be mastered before depositing thin films. Different ways exist to heat up the glass substrate such as the use of halogen lamps or the utilization of a hot plate [4]. In the present work, the heating provided by a hot plate is investigated previously to all deposition considerations, with the aim of having a better knowledge of its temperature values. For this purpose, among temperature measurement techniques, infrared thermometry has been considered as it is a convenient non-contact temperature measurement way to determine the temperature mapping. After having exposed the thermographic method employed, the experimental set up is presented. The different stages leading to the hot plate temperature evaluation are then described and the obtained temperature results are discussed.

2. Quantitative thermographic method

Infrared thermometry utilizes the spectral intensity of thermal radiation from the target surface to infer surface temperature, measured on a standardized bandwidth $\Delta\lambda$ of any radiation thermometer. Four components contribute to the measured spectral intensity $L_{\Delta\lambda}$. They lead to apparent temperature $T_{app.}$ as:

$$L_{\Delta\lambda}\left(T_{app.}\right) = L_{\Delta\lambda,e}\left(T\right) + L_{\Delta\lambda,refl.}\left(T_{back.}\right) + L_e + L_{atm.} \qquad (1)$$

where

$L_{\Delta\lambda,e}\left(T\right)$ is the intensity of radiation emitted from the target at surface temperature T;

$L_{\Delta\lambda,refl.}\left(T_{back.}\right)$ is the intensity of radiation emitted from the surroundings at temperature $T_{back.}$ and reflected by the target surface;

L_e is the intensity of radiation emitted from the target reflected by the surroundings and then the target itself;

$L_{atm.}$ results on combined effect of atmospheric scattering and absorption (H_2O, CO_2, dust particles, etc).

The measured intensity is referenced to that of a perfect absorber and perfect emitter, a blackbody, whose spectral intensity is given by the Planck distribution:

$$L^0_{\Delta\lambda}(T) = \int_{\Delta\lambda} L^0(\lambda, T)d\lambda \approx \Delta\lambda \times \frac{c_1}{\left(\bar{\lambda}\right)^5\left(e^{\frac{c_2}{\bar{\lambda}T}} - 1\right)} \quad (2)$$

where $c_1 = 1.19 \times 10^8\ W\mu m^4 m^{-2} sr^{-1}$, $c_2 = 1.439 \times 10^4\ \mu mK$ and $\bar{\lambda}$ is the average wavelength relative to radiation thermometer bandwidth $\Delta\lambda$. The spectral emissivity $\varepsilon_{\Delta\lambda}$ is the ratio of radiation intensity emitted by a real surface to the one by a blackbody at the same temperature:

$$\varepsilon_{\Delta\lambda} = \frac{L_{\Delta\lambda,e}(T)}{L^0_{\Delta\lambda}(T)} \quad (3)$$

If the target area is relatively small compared to its surroundings, the latter behaves as a large blackbody enclosure that is capable of absorbing all incoming radiation. Consequently, the term L_e in Eq. (1) can be neglected. The atmospheric scattering term $L_{atm.}$ is significant only over narrow wavelength bands and negligible elsewhere. Excluding those atmospheric scattering bands, the intensity of radiation measured from an opaque surface can be simplified as:

$$L_{\Delta\lambda}\left(T_{app.}\right) \approx L_{\Delta\lambda,e}\left(T\right) + L_{\Delta\lambda,refl.}\left(T_{back.}\right) = \varepsilon_{\Delta\lambda} L^0_{\Delta\lambda}(T) + \rho_{\Delta\lambda} L^0_{\Delta\lambda}(T_{back.}) \quad (4)$$

where $\rho_{\Delta\lambda}$ is the spectral reflectivity of the target surface, which is the fraction of radiation intensity from the blackbody surroundings at temperature $T_{back.}$ that is reflected by the target surface. For a diffuse opaque surface, Kirchhoff's law and energy conservation yield to $\rho_{\Delta\lambda} = 1 - \varepsilon_{\Delta\lambda}$. This leads to the following commonly known expression for the measured radiation intensity of an opaque target surface:

$$L_{\Delta\lambda}\left(T_{app.}\right) = \varepsilon_{\Delta\lambda} L^0_{\Delta\lambda}(T) + (1 - \varepsilon_{\Delta\lambda}) \times L^0_{\Delta\lambda}(T_{back.}) \quad (5)$$

Knowing $\varepsilon_{\Delta\lambda}$ and background temperature, Eq. (5) enables the determination of target surface temperature T from the measured spectral intensity. Regardless of the method used, Eq. (5) shows that accurate temperature measurement requires a thorough understanding of the spectral emissivity characteristics of the target surface. Numerical values of spectral emissivity can be extracted from Eq.5 as:

$$\varepsilon_{\Delta\lambda} = \frac{L_{\Delta\lambda}\left(T\right) - L^0_{\Delta\lambda}(T_{back.})}{L^0_{\Delta\lambda}(T) - L^0_{\Delta\lambda}(T_{back.})} \quad (6)$$

It implies the knowledge of each involved temperature and the calibration curve of radiation thermometer. Supposing that T is the target temperature surface, then the equivalent blackbody radiation intensity can be found in term of numerical levels using the calibration curve of the camera. The same way, apparent temperature gives equivalent measured radiation intensity, and background temperature gives the equivalent environment radiation intensity. Spectral emissivity is then calculated by using Eq. (6). From varying temperature target, it is also possible to map spectral emissivity on large temperature ranges.

3. Experimental set up

As our aim is to know the hot plate temperature with accuracy before all deposition considerations, the hot plate is placed so as to determine the radiation intensities and temperatures in Eq. (5). The experimental set up done for these determinations is shown on figure 1. The considered hot plate is made of aluminium nitride (AlN). Its area is 75 x 25 mm² and its thickness is of 3 mm. The plate is heated by embedded resistive wires. A type K thermocouple is also embedded in the plate. Both the electrical power and the temperature can be controlled by means of a Proportional Integral Derivative (PID) controller. The whole equipment, hot plate and regulation system, is commercialised by the Watlow company.

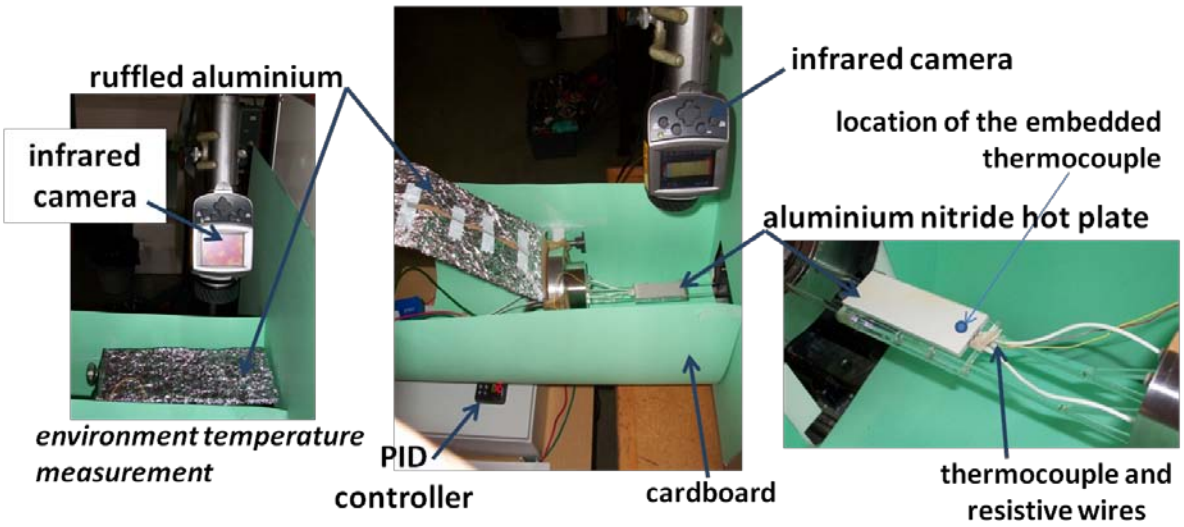

Fig. 1. *Experimental set up.*

The hot plate is placed in a surrounding cardboard in order to have a homogeneous environment. Temperatures are evaluated by means of an IRFPA camera placed vertically to the hot plate. The camera is a commercial one type FLIR E300, measuring in the long wave infrared (LWIR) domain [8 µm, 14 µm] with 320 × 240 detectors. The calibration camera was done on two ranges [-20°C, 180°C] and [80°C, 500°C]. The radiation intensity mapping of the hot plate is indeed taken with the camera for setpoint temperatures given by the K type thermocouple in the range of 40°C up to 540°C by 20°C steps.

4. Calibration curve of the camera

Calibration refers to the sets of operations which establish the relationship between the spectral radiation absorbed by each detector of an IRFPA camera (camera level) and the corresponding known value of spectral blackbody radiation emitted by the source at temperature T. An IRFPA camera is typically calibrated over a range of known temperatures. The relationship between the camera level and the blackbody temperatures constitutes the calibration curve of the camera. Calibration curve can be restored if one compares on the same graph the apparent temperature and the associated numerical level. It is then obtained by fitting data using a four degree polynomial function. The results are depicted on figure 2 for [-20°C, 120°C] temperature range.

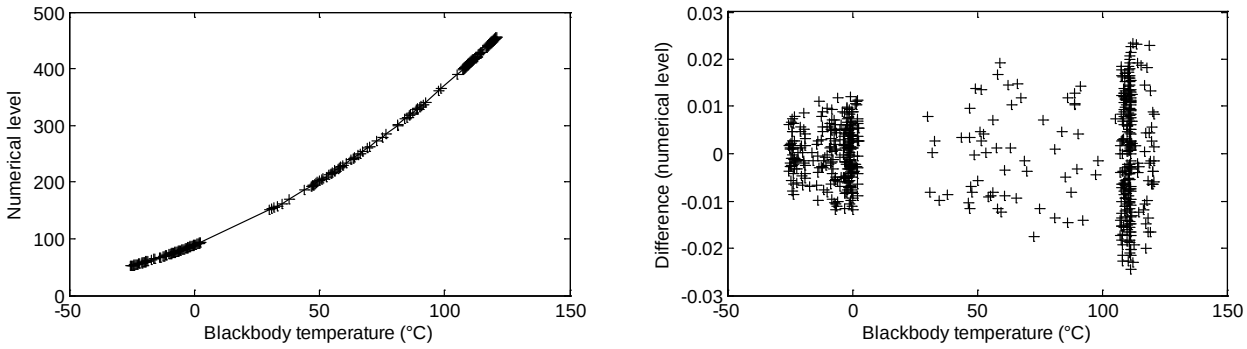

Fig. 2*. Four degree polynomial calibration curve ranging from -20°C to 120°C.*
Left picture: data (cross) and curve fit (line). Right picture: difference between data and curve fit.

Maximum residual difference is about ±0.03 levels along the temperature range. Compared to a minimum sensitivity of 2.6 levels/°C, the error made during transcription is less than 0.01°C over the entire range. Similar process is applied on the second temperature range [80°C, 500°C].

5. Emissivity calculation

The thermocouple which equips the aluminium nitride hot plate gives bulk and then surface temperature close to it. Its location is indicated on the right part of figure 1. The supplied power via the PID controller allows us to stabilize the temperature from 40°C to 540°C with 20°C steps. For each stabilized temperature, we recorded apparent, surface and background average temperatures within the areas shown on figure 3. In our case, the hot plate surface material happens not to be the same on the surface of the whole plate. There are three different material surfaces as can be seen on figure 3. To our good luck, the material surface above the thermocouple appears to be an excellent emitter. The surface temperature is then recorded on this area. Its effective emissivity is close to 1 since insignificant error is noted when we compare thermocouple and apparent temperatures. This surface material is probably an aluminium oxide thin film well known for having high effective emissivity [5]. This aluminium oxide film was certainly formed during the sintering process. The same material is present on the other end of the plate.

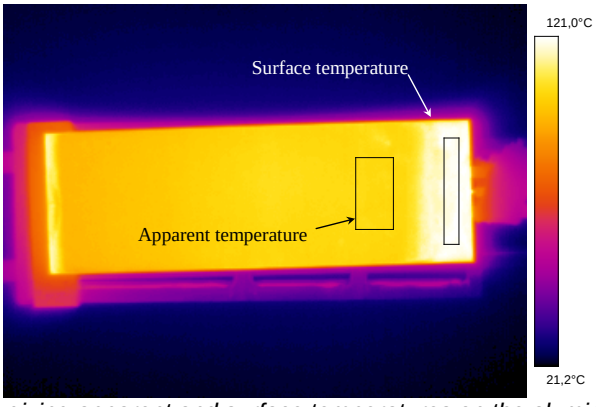

Fig. 3. *Analysis areas giving apparent and surface temperatures on the aluminium nitride plate. The two strips at the ends of the plate appear to be high emissivity emitter.*

The background temperature is recorded by means of a rigid ruffled aluminium foil according to ASTM WK21204 standard [6] which covers entirely the plate (see the left picture of figure 1).

Since we dispose of each temperature, it is possible to calculate IR camera levels associated by using the calibration curves of figure 2 and finally compute spectral emissivity given by Eq. 6. For clarity, we forget $\Delta\lambda$ index since it is now implicit that it concerns LWIR standard band. Uncertainty on spectral LWIR emissivity can be evaluated using Eq. 7:

$$\frac{\Delta\varepsilon}{\varepsilon} = \frac{\Delta L + \Delta L^0(T_{back.})}{L - L^0(T_{back.})} + \frac{\Delta L^0(T) + \Delta L^0(T_{back.})}{L^0(T) - L^0(T_{back.})} \qquad (7)$$

Levels are determined with an absolute precision due to absolute uncertainty on radiometric temperature. Level uncertainties are deduced from $\Delta L(T) = s \times \Delta T$ where s is the sensitivity in levels/°C. Radiometric temperature uncertainties are previously evaluated using a blackbody calibrator on the range [40°C, 300°C] and show an uncertainty of less than ±0.5% on the camera range 1 [-20°C,120°C] and of less than ±0.7% for the other camera range 2 [80°C, 500°C]. Background temperature is evaluated within arbitrary ±1°C. The obtained normal emissivity results are provided on figure 4 for surface temperatures going from 40°C up to 120°C for both the camera ranges.

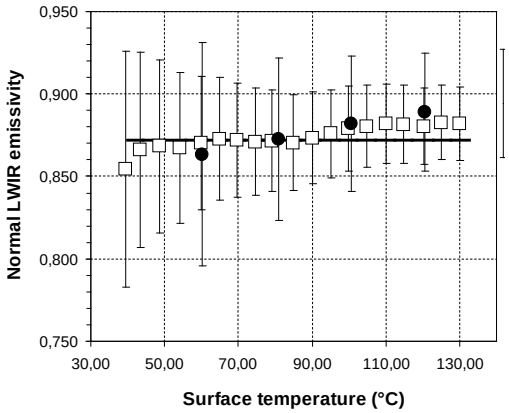

Fig. 4. *Normal LWIR emissivity of sintered AlN plate. Square marks: camera range [-20°C, 120°C]; round marks: camera range [80°C, 500°C]. Solid line: emissivity obtained from classical ellipsometry method on AlN amorphous thick film.*

A good agreement is found by taking into account the uncertainty of the two ranges. The emissivity value of aluminium nitride had been evaluated in another way by a classical method of ellipsometry which allows to find complex refractive indexes [7]. Considering the evaluated optical characteristics of aluminium nitride amorphous thick films, aluminium nitride emissivity is about 0.872. Thus, present emissivity measurements are in very good agreement with this standard method for temperatures between 40°C and 120°C. However, no temperature dependence is envisaged. Extending the emissivity determination to the second temperature range [80°C, 500°C], the emissivity is found temperature dependent as represented on the figure 5 graph. Taking into account the porosity of sintered aluminium nitride in the order of 5 to 10 µm [8,9], we suggest that typical porosity interacts with wavelength above Wien's temperature of 30°C. Above such temperature, sintered aluminium nitride tends to a perfect emitter with a total emissivity getting close to 1.

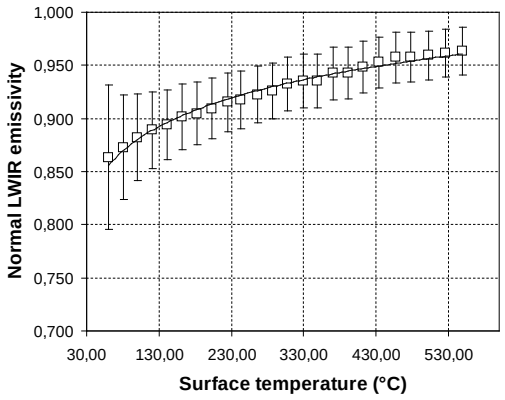

Surface temp. / °C	Emissivity	Uncertainty / ±	Surface temp. / °C	Emissivity	Uncertainty / ±
60,3	0,863	0,039	307,7	0,933	0,018
80,8	0,873	0,030	329	0,935	0,018
100,5	0,882	0,025	348	0,935	0,017
120,6	0,889	0,023	370,3	0,942	0,017
141,8	0,894	0,021	391,6	0,943	0,017
161,9	0,902	0,020	411,7	0,948	0,017
182,5	0,905	0,020	433,9	0,953	0,017
203,1	0,909	0,019	456,6	0,957	0,017
225,4	0,915	0,019	477,6	0,958	0,016
243,4	0,918	0,019	501,8	0,959	0,016
266,8	0,923	0,018	525,8	0,961	0,016
286,4	0,926	0,018	548,6	0,963	0,016

Fig. 5. *. Temperature dependence of normal LWIR emissivity of AlN plate with the corresponding found data.*

6. Temperature profiles

Since the normal emissivity is known, the true hot plate temperature can be deduced. The temperatures are first analyzed on several segments taken on the hot plate longitudinal midline as indicated on figure 6. The apparent temperatures from segment 2 are corrected using normal emissivity and the background temperature following Eq.5. Segments 1 and 3 are supposed to give the exact surface temperature since the surface material is a quasi-perfect emitter. A good agreement at the segment extremities is then expected. Abscissa is normalized to 75 mm corresponding to the plate length. Temperature values are secondly looked in the transverse midline of the plate and normalized to 25 mm corresponding to the plate width.

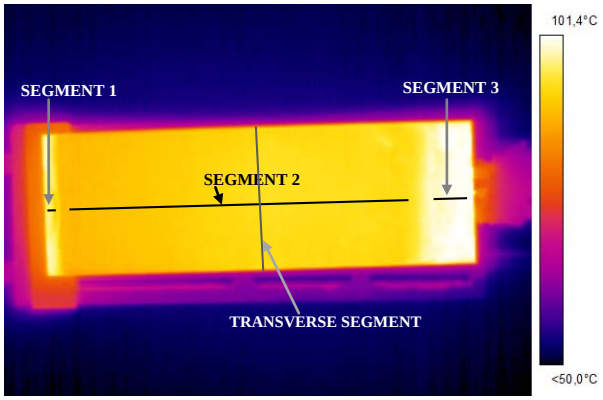

Fig. 6. *Analyzed segments: 1, 2 and 3 in the longitudinal direction and the one in the transverse direction.*

Uncertainty on absolute temperature is evaluated using $\Delta T = \Delta L^0(T)/s$ where $\Delta L^0(T)$ is the uncertainty on the blackbody emitter level $L^0(T)$ given by Eq.8:

$$\frac{\Delta L^0(T)}{L^0(T)} = \frac{\Delta L(T_{app})}{L(T_{app})} + 2\times\frac{\Delta\varepsilon}{\varepsilon} + 2\times\frac{\Delta L^0(T_{back.})}{L^0(T_{back.})} \qquad (8)$$

The absolute temperature uncertainties are unchanged as in the emissivity calculation (see part 5). The temperature results are shown on figure 7 for the longitudinal direction and on figure 8 for the transversal one for several setpoint temperatures going from 100°C up to 500°C. The calculated uncertainty bars with Eq. (8) are indicated. The temperature differences compared to the mean value are displayed on the right part of figures 7 and 8.

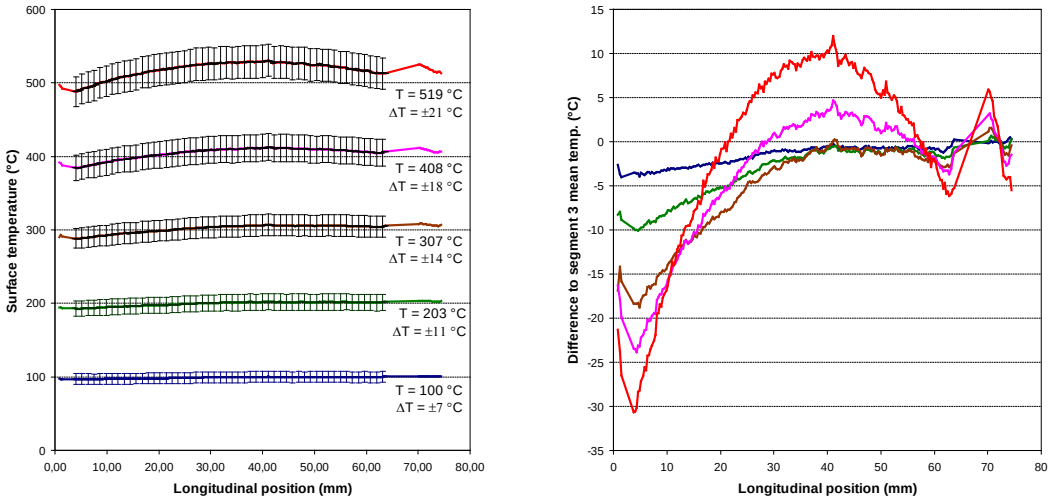

Fig. 7. *Left: lengthwise temperature profiles with the uncertainty bars.*
Right: temperature difference compared to segment 3 mean temperature.

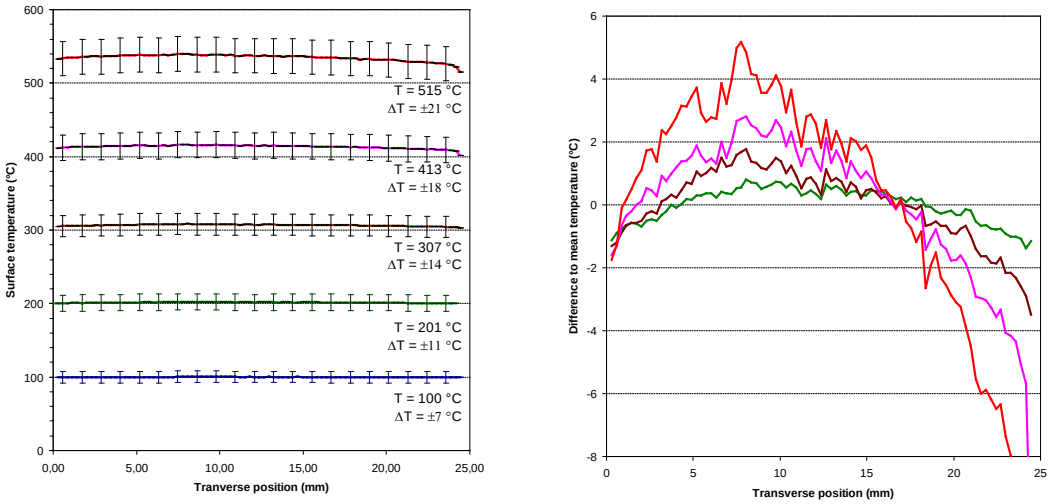

Fig. 8. *Left: transverse temperature profiles with the uncertainty bars. Right: difference with regard to mean temperature.*

A good agreement is verified at the segment extremities for the lengthwise temperature profiles. The temperature uncertainty increases when the temperature raises mainly because of the emissivity uncertainty. However, in percentage it decreases with temperature. The uncertainty is found in the order of 8% for the considered lower temperatures and up to 4% for the upper ones. So, the method is interesting to evaluate high temperature.

The temperature differences increase when the hot plate overall temperature is more important. The difference in the longitudinal direction is bigger than the one in the transverse direction because the length is equal to three times the width of the hot plate. Nevertheless, in terms of percentage, the temperature difference is inferior to 8% of the mean temperature value for the lengthwise midline and inferior to 2.5% for the transverse one. So, a good homogeneity is found for the hot plate temperature.

7. Conclusion

The temperature of an aluminium nitride hot plate which can be used for spray CVD (Chemical Vapour Deposition) has been determined by a thermographic method. First, the calibration curve of the commercial infrared camera utilized was acquired. The normal emissivity of the aluminium nitride of the hot plate was then found by measuring apparent, surface and background temperatures in the range [40°C, 540°C]. The emissivity values are in good agreement with the measured one by the classical method of ellipsometry for temperatures inferior to 120°C. The aluminium nitride emissivity versus the temperature is also obtained for temperatures going up to 540°C. This dependence can be most certainly explained by the porosity of the sintered aluminium nitride hot plate. Knowing the emissivity with a precision better than 3%, the true temperature profiles were deduced for both the mid longitudinal and transverse directions of the hot plate. The temperature uncertainty is as well calculated with an accuracy ranging from 8 to 4% for high temperatures. Indeed, the uncertainty decreases in percentage when the hot plate temperature increases which makes it worthwhile using the present thermographic approach for high temperature evaluation. Finally, good temperature homogeneity is verified with temperature differences all inferior to 8% of the mean temperature. So, our next step is thin film deposition with a glass substrate laid on the hot plate. Numerical simulation is also another interesting perspective since the aluminium nitride emissivity values are known with the temperature.

REFERENCES

[1] Lavernia E.J. and Wu Y., “Spray atomization and deposition”, Editions Wiley, 1996.
[2] Zhou Z.B., et al., “Preparation of indium tin oxide films and doped tin oxide films by an ultrasonic spray CVD process”, Applied Surface Science, 172(3-4), (2001) 245-252.
[3] de la L. Olvera I.M., Gómez H. and Maldonado A., "Doping, vacuum annealing, and thickness effect on the physical properties of zinc oxide films deposited by spray pyrolysis”, Solar Energy Materials and Solar Cells, 91(15-16), (2007) 1449-1453.
[4] Girtan M., Logerais P.O. and Bouteville A., “Substrate thermal profiles in spray-CVD reactor”, Journal of Optoelectronics and Advanced Materials, 8(1), (2006) 144-147.
[5] White F.M., “Heat transfer”, Addison-Wesley, Reading, MA, 1984.
[6] ASTM Standard C33, 2003, "Specification for Concrete Aggregates," ASTM International, West Conshohocken, PA, 2003, DOI: 10.1520/C0033-03, www.astm.org.
[7] Palik E.D., “Handbook of Optical Constants of Solids”, Academic Press, New York, 1998.
[8] Ivanov S.N. et al., “Thermophysical properties of aluminium nitride ceramic”, Physics of the Solid State, 39(1), (1997) 81-83.
[9] Sciti D., Winterhalter F.and Bellosi A., “Oxidation behaviour of a pressureless sintered AlN-SiC composite”, Journal of Materials science, 39, (2004) 6965-6973.